# Synthesis, Isomer Characterization, and Anti-Inflammatory Properties of Nitroarachidonate†

Andrés Trostchansky,‡ José M. Souza,‡ Ana Ferreira,§ Mariana Ferrari,§ Fabiana Blanco,‡ Madia Trujillo,‡ Diego Castro,|| Hugo Cerecetto,|| Paul R. S. Baker,⊥ Valerie B. O'Donnell,# and Homero Rubbo*,‡

*Department of Biochemistry and Center for Free Radical and Biomedical Research, Faculty of Medicine, and Departments of Immunology and Organic Chemistry, Faculty of Chemistry/Sciences, University of the Republic, Montevideo, Uruguay, Department of Pharmacology, University of Pittsburgh School of Medicine, Pennsylvania, and Department of Medical Biochemistry and Immunology, Cardiff University, Cardiff, U.K.*

*Received December 27, 2006; Revised Manuscript Received February 15, 2007*

ABSTRACT: Nitrated fatty acids (nitroalkenes) have been recently detected and quantified in cell membranes and human plasma. However, nitration of arachidonate (AA), that could redirect AA-dependent cell signaling pathways, has not been studied in detail. Herein, we synthesized and determined for the first time the isomer distribution of nitroarachidonate ($AANO_2$) and demonstrate its ability to modulate inflammation. Synthesis of $AANO_2$ was achieved by AA treatment with sodium nitrite in acidic conditions following HPLC separation. Mass spectrometry (MS) analysis showed the characteristic MS/MS transition of $AANO_2$ (*m*/*z* 348/301). Moreover, the IR signal at 1378.3 $cm^{-1}$ and NMR studies confirmed the presence of mononitrated nitroalkenes. Positional isomer distribution was determined by NMR and MS fragmentation with lithium; four major isomers (9-, 12-, 14-, and 15-$AANO_2$) were identified, which exhibited key anti-inflammatory properties. These include their ability to release biologically relevant amounts of nitric oxide, induce cGMP-dependent vasorelaxation, and down-regulate inducible nitric oxide synthase (NOS2) expression during macrophage activation, providing unique structural evidence and novel regulatory signaling properties of $AANO_2$.

The unique structure of arachidonic acid ((5*Z*,8*Z*,11*Z*,14*Z*)-icosa-5,8,11,14-tetraenoic acid, AA[1]), a 20-carbon polyunsaturated fatty acid with four double bonds, enables it to be a precursor of potent signaling molecules, i.e., prostaglandins, thromboxanes, and isoprostanes *via* enzymatic and nonenzymatic oxidative pathways (*1*−*7*). Nitric oxide (•NO) represents a key signaling mediator of inflammation linked with prostanoid biosynthesis (*2*). During PGHS catalysis, AA derived-radicals (AA•) as well as tyrosyl radicals are formed being potential targets for •NO reactivity thus influencing enzyme activity (*8*, *9*).

We have postulated that •NO is a major lipophilic antioxidant due to its chain-breaking lipid oxidation capacity (*10*−*12*). Nitric oxide and •NO-derived species (NOx) reactions with oxidized fatty acids result in the formation of a wide variety of oxidized and nitrated fatty acids (*5*, *7*, *12*−*16*). Nitroalkenes (i.e., nitrolinoleate, $LNO_2$, and nitrooleate, $OANO_2$) have been recently detected and quantified in red blood cells and urine as well as in plasma from healthy and hypercholesterolemic patients (*16*−*18*). Some of the biological properties of $LNO_2$ and $OANO_2$ include their capacity to trigger peroxisome proliferator-activated receptor $\gamma$ (PPAR$\gamma$) signaling pathways (*16*, *19*), releasing •NO in aqueous milieu (*13*, *20*) and promoting endothelium-independent vessel relaxation (*14*).

Nitration of AA by inflammatory stimuli could divert the "normal metabolic pathways" of AA to gain novel responses. Nitrogen dioxide ($^{\bullet}NO_2$) or peroxynitrite isomerizes AA to *trans*-AA in a specific process that could be of significance in pathologies related with an increase in NOx, including inflammatory diseases, endotoxemia, and cigarette smoke (*21*). Hydrophobic membranes may facilitate reactions where •NO, $^{\bullet}NO_2$, AA•, and arachidonyl peroxyl radicals (AAOO•) are likely to be simultaneously present, which occurs in many cell types such as macrophages or endothelium under oxidative/nitrative stress conditions. The half-life of AAOO•

† This work was supported by grants from Fondo Clemente Estable, Uruguay, to A.T., Wellcome Trust to H.R. and V.B.O., and Programa de Desarrollo Tecnológico, Uruguay, FOGARTY-NIH, and the Guggenheim Foundation to H.R. A.T. was partially supported by a fellowship from Programa de Desarrollo de Ciencias Básicas (PEDECIBA, Uruguay).

* Address correspondence to this author at Departamento de Bioquímica, Facultad de Medicina, Avda. General Flores 2125, Montevideo, Uruguay. Phone: (5982) 924-9561. Fax: (5982) 924-9563. E-mail: hrubbo@fmed.edu.uy.

‡ Faculty of Medicine, University of the Republic.

§ Department of Immunology, Faculty of Chemistry/Sciences, University of the Republic.

|| Department of Organic Chemistry, Faculty of Chemistry/Sciences, University of the Republic.

⊥ University of Pittsburgh School of Medicine.

# Cardiff University.

[1] Abbreviations: AA, arachidonic acid; •NO, nitric oxide; $AANO_2$, nitroarachidonate; TLC, thin-layer chromatography; cPTIO, 2-(4-carboxyphenyl)-4,4,5,5-tetramethylimidazoline-oxyl-3-oxide; DAF-2DA, 4,5-diaminofluorescein diacetate; MeOH, methanol; RP-HPLC, reverse phase HPLC; MS, mass spectrometry; ESI MS/MS, electrospray ionization tandem mass spectrometry; MRM, multiple reaction monitoring; *m*/*z*, mass to charge ratio; EPI, enhanced product ion analysis; PGHS, prostaglandin endoperoxide H synthase; SOD, superoxide dismutase; sGC, soluble guanylate cyclase; ODQ, 1*H*-[1,2,4]oxadiazole-[4,3-*a*]quinoxalin-1-one; NOS2, inducible nitric oxide synthase.

10.1021/bi602652j CCC: $37.00 
Published on Web 03/21/2007

is 0.1−0.2 s, sufficiently long for the reaction with NOx to occur, leading to arachidonyl peroxynitrites (AAOONO)/nitrates that could rearrange into nitroarachidonate ($AANO_2$), nitrohydroxyarachidonate ($AA(OH)NO_2$), and nitro-epoxy-AA (*12*, *21*, *22*). Thus, $^{\bullet}NO$ and $^{\bullet}NO_2$ may modulate AA oxidation through the formation of $AANO_2$ that could potentially function as a novel signaling molecule and a specific biological marker of inflammation. Herein, we synthesized $AANO_2$ by acidic nitration, determined its isomer distribution, chemical and biological properties, and its ability to modulate inducible nitric oxide synthase (NOS2) expression during macrophage activation.

## EXPERIMENTAL PROCEDURES

*Materials.* Arachidonic acid was purchased from Nu-Check Prep (Elysian, MN). Silica gel HF thin-layer chromatographic (TLC) plates were obtained from Analtech. The solvents used in syntheses were HPLC grade; solvents for mass spectrometry were obtained from Pharmco (Brookfield, CT). 2-(4-Carboxyphenyl)-4,4,5,5-tetramethylimidazoline-oxyl-3-oxide (carboxy-PTIO) and NOC-18 were from Dojindo Laboratories, Japan. 4,5-Diaminofluorescein diacetate (DAF-2DA) was from Alexis, U.S.A. Lithium acetate, $NaNO_2$, LPS, and Interferon-$\gamma$ were obtained from Sigma Chemical (St. Louis, MO).

*Synthesis of $AANO_2$.* Nitration of AA was performed as previously described (*7*, *16*, *23*−*25*) with modifications: AA was treated with $NaNO_2$ at a 1:1 molar ratio under continuous stirring at 25 °C for an hour and pH adjusted to 3.0. The reaction was stopped by solvent extraction with ethyl acetate/NaCl (1:2, v/v); the organic phase was collected and evaporated, and lipid products were dissolved in methanol (MeOH). $AANO_2$ positional isomers were isolated by reverse phase HPLC (RP-HPLC) using a 250 × 2 mm C18 Phenomenex Luna column (3 $\mu$M particle size), and lipids were eluted using a solvent system consisting of A ($H_2O$ containing 0.05% formic acid) and B ($CNCH_3$ containing 0.05% formic acid) under the following gradient conditions: 35% B (0−10 min); 35−100% B (10−35 min); and 100−35% B (35−45 min). The elution of the lipid oxidized and nitrated products was followed by UV detection at 215 and 274 nm (*7*, *16*, *22*). Fractions were collected, extracted using the method of Bligh and Dyer (*26*), and stored at −20 °C in MeOH. Identification of $AANO_2$ products was performed by electrospray ionization tandem mass spectrometry (ESI MS/MS) as explained below. The presence of nitrated derivatives of AA in the reaction mixture and the absence of AA or AA-oxidized products in the purified fractions were also determined by TLC using silica gel HF plates developed in a solvent system consisting of hexane/diethyl ether/acetic acid (80/20/1, v/v). Lipid products were visualized by UV and under iodine atmosphere (*13*, *27*). Yields of $AANO_2$ (as mixture of four isomers, see below) were less than 10%.

*Structural Characterization of $AANO_2$.* Electrospray ionization tandem mass spectrometry was performed for qualitative analysis of $AANO_2$ using a hybrid triple quadrupole/linear ion trap mass spectrometer (QTRAP 2000, Applied Biosystems/MDS SCIEX). Reaction mixtures or purified fractions were injected in MeOH at a flow of 10 $\mu$L/min with the instrument operated in the negative ionization mode. The skimmer potential was −50 V and desolvation temperature set to 350 °C; for daughter ion analysis, the collision energy was 20 eV. To characterize $AANO_2$, lipids were separated by RP-HPLC using a 150 × 2 mm C18 Phenomenex Luna column (3 $\mu$m particle size) and eluted from the column using a gradient solvent system consisting of A ($H_2O$ containing 0.1% $NH_4OH$) and B ($CNCH_3$ 0.1% $NH_4OH$) under the following gradient conditions: 35% B (0−5 min); 35−100% B (5−25 min); and 100−35% B (25−35 min). Detection of $AANO_2$ was performed using the multiple reaction monitoring (MRM) scan mode by reporting molecules that undergo the neutral loss of the nitro group consistent with a *m*/*z* 348/301 MRM transition (*16*). The presence of hydroxy derivatives of $AANO_2$ ($AA(OH)NO_2$) or AA were also analyzed through the *m*/*z* 366/319 (neutral loss of the $NO_2$ group) (*16*) and *m*/*z* 303/259 (loss of $CO_2$) (*28*) mass transitions, respectively. Concurrent with MRM determination, enhanced product ion analysis (EPI) was performed to generate characteristic fragmentation patterns of eluting species with a precursor mass of *m*/*z* 348. Quantitation of $AANO_2$ was performed by HPLC ESI MS/MS using $[^{13}C_{18}]OANO_2$ (MRM transition monitored: *m*/*z* 344/297). The areas under $AANO_2$ and $[^{13}C_{18}]OANO_2$ peaks were integrated, the ratios of the analyte to internal standard areas were determined, and $AANO_2$ was quantitated using Analyst 1.4 quantitation software (Applied Biosystems/MDS Sciex). The identification of $AANO_2$ as a nitro derivative, and not a nitrite one, was also evaluated by infrared spectroscopy (IR) as previously (*14*, *17*), accumulating 40 scans between 600 and 4000 $cm^{-1}$.

*Analysis of $AANO_2$ Positional Isomers.* The position of the nitro group in AA was determined by ESI MS/MS and NMR. For MS/MS determination, $AANO_2$ was injected to the Q-Trap in MeOH containing 5 mM lithium acetate and the corresponding products were determined in the positive-ion mode. NMR spectroscopic analysis of $AANO_2$ involved $^1H$, $^{13}C$, bidimensional COSY, HMQC, and HMBC experiments recorded in $CDCl_3$ (Bruker DPX-400 instrument).

*Nitric Oxide Releasing Activity of $AANO_2$.* The capacity of $AANO_2$ to release $^{\bullet}NO$ was evaluated by (a) oxyhemoglobin (oxyHb) oxidation (*13*), recording the spectrum from 400 to 700 nm in the presence of $AANO_2$ repetitively at 5 min intervals; (b) by electrochemical detection using a $^{\bullet}NO$-selective electrode (WPI Instruments, Ann Arbor, MI, ref *10*) in the absence or presence of superoxide dismutase (SOD); and (c) by electron paramagnetic resonance (EPR), using the specific scavenger of $^{\bullet}NO$ by 2-(4-carboxyphenyl)-4,4,5,5-tetramethylimidazoline-oxyl-3-oxide (carboxy-PTIO, $k = 10^4\ M^{-1}\ s^{-1}$) (*13*, *20*, *29*). The Bruker EMX spectrometer was tuned as follows: frequency, 9.76 GHz; modulation frequency, 100 kHz; modulation amplitude, 0.5 G; receiver gain, 2.83 × $10^3$; time constant, 1.28 ms; sweep time, 5.24 s; center field, 3479 G; sweep width, 80.64 G; power, 19.97 mW; scan parameter, 16 scans.

*Cell Culture.* J774.1 murine macrophage-like cells (ATCC, U.S.A.) were maintained by passage in DMEM containing 4 mM L-glutamine, and supplemented with 10% heat-inactivated fetal calf serum (FCS).

*Biological Activity of $AANO_2$.* Confluent monolayers of J774.1 cells were activated by exposing to 3 $\mu$g/mL *Escherichia coli* lipopolisacharide (LPS, serotype 0127:B8, Sigma) plus 400 U/mL murine recombinant interferon-

gamma (IFN$\gamma$, Sigma). In parallel, cells were cultured in the absence of stimulus or in the presence of NOC-18 as controls. Experiments were performed in medium (DMEM-10%FCS) with vehicle, AA or $AANO_2$. After 6 h incubation, supernatants were discarded, cells were washed, and inducible nitric oxide synthase (NOS2) expression was assessed by Western blot analysis using a polyclonal anti-NOS2 antibody (Sigma Chemical) or by monitoring the release of $^{\bullet}NO$ using the cell-permeable fluorescence indicator 4,5-diaminofluorescein diacetate (DAF-2DA). Briefly, cells were incubated in medium containing 5 $\mu$M DAF-2DA and 1 mM L-arginine and fluorescence ($\lambda_{excitation}$ = 495 nm, $\lambda_{emission}$ = 515 nm) was recorded during 1 h using a FLUOstar-OPTIMA fluorimeter (BMG Labtechnologies GmbH, Germany). For analyzing $AANO_2$ effects on synthesized NOS2, cells were activated for 6 h and then the translation inhibitor cycloheximide (5 $\mu$M) and $AANO_2$ were added and further incubated for 3 h, following NOS2 analysis. For vessel studies, male Wistar Kyoto rats (250−300 g) were heparinized (100 U/mL) and after 20 min anesthetized (40 mg/kg pentobarbital ip) and the descending thoracic aorta was excised (all experimental procedures were approved by Comisión Honoraria de Experimentación Animal, Universidad de la República). Aortic rings (4 mm in length) were mounted under 2 g of passive tension in a Radnoti tissue-organ bath system containing Krebs−Henseleit solution, maintained at 37 °C and gassed with 95% $O_2$−5% $CO_2$, pH 7.4. Aortic rings were allowed to equilibrate for 1 h, precontracted with 1 $\mu$M noradrenaline (NOR), and thereafter exposed to $AANO_2$ (10 $\mu$M; ref *30*). The relaxation response, measured as the percentage of change in isometric force, was studied in the absence or presence of the soluble guanylate cyclase (sGC) inhibitor 1*H*-[1,2,4]oxadiazole[4,3-*a*]quinoxalin-1-one (ODQ, 30 $\mu$M) (*7*, *20*). For experiments with endothelium-denuded arteries, preparations were rubbed in their internal surface with a rough glass capillary. Control experiments were performed with MeOH and non-nitrated AA.

## RESULTS

*Synthesis and Purification of $AANO_2$.* Nitration of arachidonic acid was performed by AA incubation with $NaNO_2$ under acidic conditions (see Experimental Procedures); the reaction mixture was extracted and analyzed by RP-HPLC and TLC. The main oxidation product was *trans*-AA (data not shown) in accordance with previous reports (*7*). Arachidonate exhibits a *m*/*z* of 303 in the negative mode (data not shown) that changes to a *m*/*z* of 348 due to the addition of a nitro ($-NO_2$) group to the fatty acid chain. Under our experimental conditions three HPLC fractions, with UV absorbance spectrum maxima at 276 nm (data not shown), were collected (labeled as 1−3 in Figure 1A) and exhibited a *m*/*z* of 348. The presence of $AANO_2$ in these fractions was followed by LC MS/MS using the MRM scan mode following the neutral loss of the $NO_2$ group (*m*/*z* 348/301 MRM transition) and their identity confirmed by MS/MS scanning, selecting the parent ion with *m*/*z* 348 (Figure 1B). A nitrohydroxy derived product of AA (*m*/*z* 366 and *m*/*z* 366/319 MRM transition) was also identified (Figure 1C), according to Balazy, M., et al. (*7*). $AANO_2$ fractions eluted at greater acetonitrile concentration than $AA(OH)NO_2$ (Figures 1B and 1C).

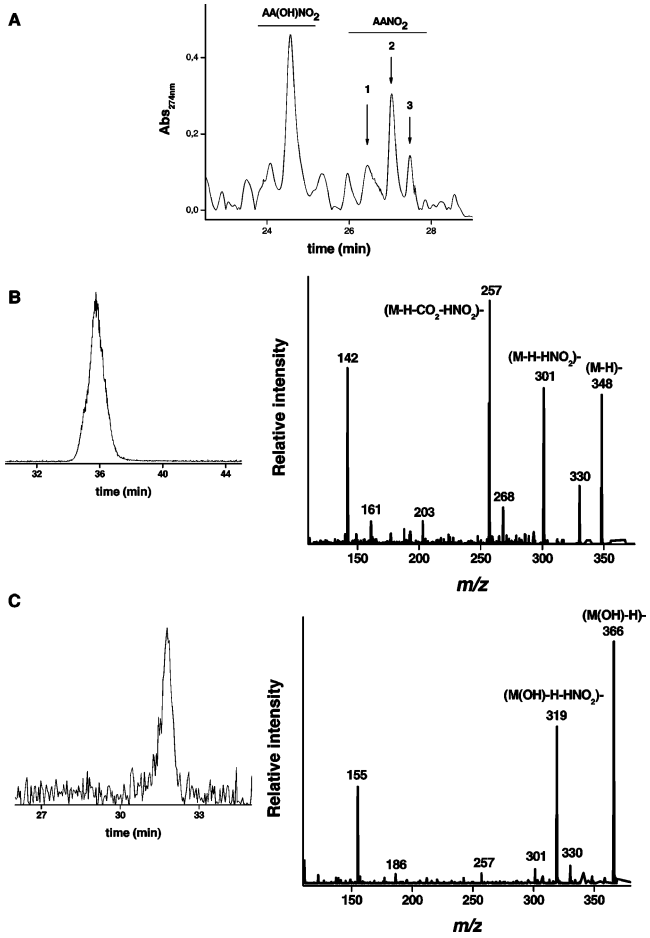


FIGURE 1: Identification and structural characterization of $AANO_2$ by HPLC ESI MS/MS. (A) AA was incubated with $NaNO_2$ at pH 3 for an hour at 25 °C; lipid products were extracted and separated by RP-HPLC. Detection was performed at 274 nm, and fractions corresponding to $AANO_2$ eluted from 26.5 to 28 min (indicated with arrows and numbered from 1 to 3). These products were also analyzed by TLC showing lower $R_f$ than AA (see Supporting Information). (B, C) Fractions from A (MRM data shown correspond to fraction 3) were obtained and identified by HPLC ESI MS/MS. Detection was performed by acquiring MRM transitions consistent with the loss of the nitro functional group: *m*/*z* 348/301 and *m*/*z* 366/319 for $AANO_2$ and $AA(OH)NO_2$, respectively (left panels). The identity of these products was also confirmed by the enhanced product ion (EPI) analysis showed in the right panels.

*NMR and IR Analysis.* Although fractions 1 to 3 exhibited MRM transitions corresponding to the presence of nitroarachidonates, the neutral loss of a 47 mass unit fragment does not distinguish between a nitro ($-NO_2$) or a nitrite ($-ONO$) functional group. To identify functional groups, HPLC-purified fractions having *m*/*z* 348 were analyzed by IR and NMR spectroscopy. The IR analysis showed the presence of a nitro derivative and disproved the presence of nitrite (AAONO) or nitrate esters products ($AAONO_2$, Table 1). Nitro bonds present a characteristic absorption in the 1310−1397 and 1548−1560 $cm^{-1}$ regions (*14*, *17*). The IR spectrum of the three HPLC-purified $AANO_2$ fractions showed the characteristic absorption of the N═O at 1370 and 1555 $cm^{-1}$ (Table 1 and Supporting Information). The presence of organic nitrites or nitrates was precluded because no absorption in the 1600−1680 $cm^{-1}$ region was observed (*14*, *17*). Further structural information was obtained from NMR experiments (Scheme 1, Table 2 and Supporting Information): (a) New protons and

Table 1: Infrared Wavenumbers ($cm^{-1}$) of $AANO_2$

| functional group | arachidonate | fraction 1[a] | fraction 2[a] | fraction 3[a] | reported data (*14*, *17*) |
|---|---|---|---|---|---|
| N═O of nitro (asym), $RNO_2$ | | 1554 | 1554 | 1555 | 1560−1548 |
| N═O of nitro (sym), $RNO_2$ | | 1368 | 1381 | 1370 | 1397−1310 |
| N═O of nitrito, RONO | | | | | 1680−1610 |
| N═O of nitrate, $RONO_2$ | | | | | 1660−1625 |
| OH of carboxylic acid | 3020 | 3026 | 3018 | 3023 | 3335−2500 |
| C═O carbonyl | 1708 | 1708 | 1709 | 1709 | 1725−1695 |
| C−H | 2922 | 2929 | 2858 | 2929 | 2850−2940 |
| C−C | 1463 | 1463 | 1460 | 1460 | 1410−1470 |

[a] Fractions 1−3 correspond to the same fractions obtained from HPLC (Figure 1A).

Scheme 1: NMR Analysis of $AANO_2$[a]

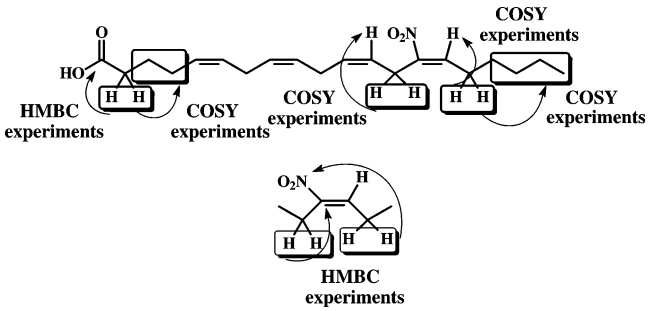


[a] $^1H$ NMR spectroscopy in addition to 2D experiments, COSY, HBMC, and HMQC analysis were performed to confirm the structure of $AANO_2$. 14-$AANO_2$ was used to exemplify.

carbons appear in the protons and carbons-olefinic region near 7 ppm and 130−150 ppm, respectively, corresponding to the new system CH═$CNO_2$. In addition, changes in the olefinic protons' integrations were observed. (b) Changes in the chemical shifts and multiplicities of the allylic protons that correlate with carbons in the 130−150 ppm regions (HMBC experiments) were observed. Moreover, COSY experiments showed the coupling of allylic protons with olefinic protons. (c) COSY experiments showed the couplings for head's and tail's protons.

*Identification of $AANO_2$ Isomers by ESI MS/MS.* $AANO_2$ fractions were analyzed by ESI MS/MS in the presence of lithium acetate. The $[M - Li]^+$ ions obtained exhibit a *m*/*z* of 356 (Figure 2 and Table 3). The presence of lithium locks the charge at the carboxy moiety and allows the cleavage directly across the nitroalkene double bond, depending on the position of the $NO_2$ group, generating two specific fragments. The fragments carrying the charge, allowing its detection by MS, corresponded to those having the carbon closer to the carboxyl group in the nitroalkene double bond. Specific patterns of collision-induced dissociation fragments for each theoretical isomer were obtained. MS/MS spectra showed the presence of the $[M - Li]^+$ ion as well as the one that suffered the neutral loss of the $NO_2$ group (*m*/*z* 309, Figure 2). From MS/MS spectra, four major isomers (Figure 2 labeled with an asterisk) were identified: 12- and 15-nitroarachidonate (*m*/*z* 203 and *m*/*z* 243, respectively) in fraction 1, the most polar one; 9-nitroarachidonate (*m*/*z* 163) in fraction 2, medium polarity; and 14-nitroarachidonate (*m*/*z* 256) in fraction 3, the less polar one. These results, in addition to the NMR data, clearly identify the nitroalkene positional isomers of $AANO_2$. Although other fragments were observed, structural analysis confirmed the absence of other isomers (data not shown).

*Biological Activity of $AANO_2$.* The capacity of $AANO_2$ to release •NO was demonstrated in parallel by oxyHb oxidation (Figure 3A) and EPR following cPTIO reduction to cPTI (black line, Figure 3B). Quantitation of •NO release from $AANO_2$ in aqueous solution was evaluated by using the •NO electrode: while not spontaneous •NO release was detected, it was observed only in the presence of SOD, probably due to the formation of superoxide ($O_2^{\bullet -}$) during the process of $AANO_2$ decay. This $O_2^{\bullet -}$ should scavenge •NO, preventing its detection by the electrode. Quantitative analysis indicated that 10 $\mu$M $AANO_2$ in the presence of SOD released •NO at a flux of 8 $\mu$mol of •NO/mmol of $AANO_2$/min (data not shown). The releasing of •NO by $AANO_2$ was also related to its vasorelaxing properties: $AANO_2$ induced vasorelaxation in an endothelium-indepen-

Table 2: Characteristic NMR Data ($CDCl_3$) Used To Elucidate $AANO_2$ Structure in Fraction 3[a]

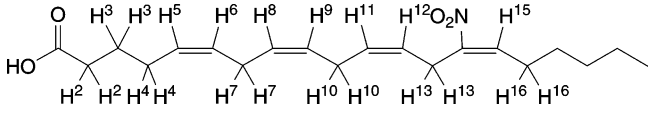

| | | | relevant correlations in | |
|---|---|---|---|---|
| proton | $^1H$ (multiplicity, *J* (Hz)) | $^1H-^1H$ COSY | $^1H-^{13}C$ HMQC | $^1H-^{13}C$ HMBC |
| H-15 | 7.14 (t, 8.0) | 2.28 | 135.00 | 150.00 (C14), 48.20 |
| H-5,6,8,9,11 | 5.58−5.35 (m) | 2.95−2.75, 2.18 | 131.00−127.00 | |
| H-12 | 5.35−5.30 (m) | 5.58−5.35, 3.40 | | 150.00, 131.00−127.00, 48.20 |
| H-13 | 3.40 (d, 7.4) | 5.35−5.30 | 48.20 | 150.00, 135.00, 131.00−127.00 |
| H-7,10 | 2.95−2.75 (m) | 5.58−5.35 | | 131.00−127.00 |
| H-2 | 2.40 (t, 7.4) | 1.76 | 33.00 | 176.00, 27.00 |
| H-16 | 2.28 (q, 8.0) | 7.14, 1.40−1.20 | | 150.00, 135.00 |
| H-4 | 2.18 (m) | 5.58−5.35, 1.76 | 27.00 | 131.00−127.00 |
| H-3 | 1.76 (m) | 2.40, 2.18 | | |

[a] Fraction 3 corresponds to the same fraction purified by HPLC in Figure 1A. Data for fractions 1 and 2 are shown as Supporting Information.

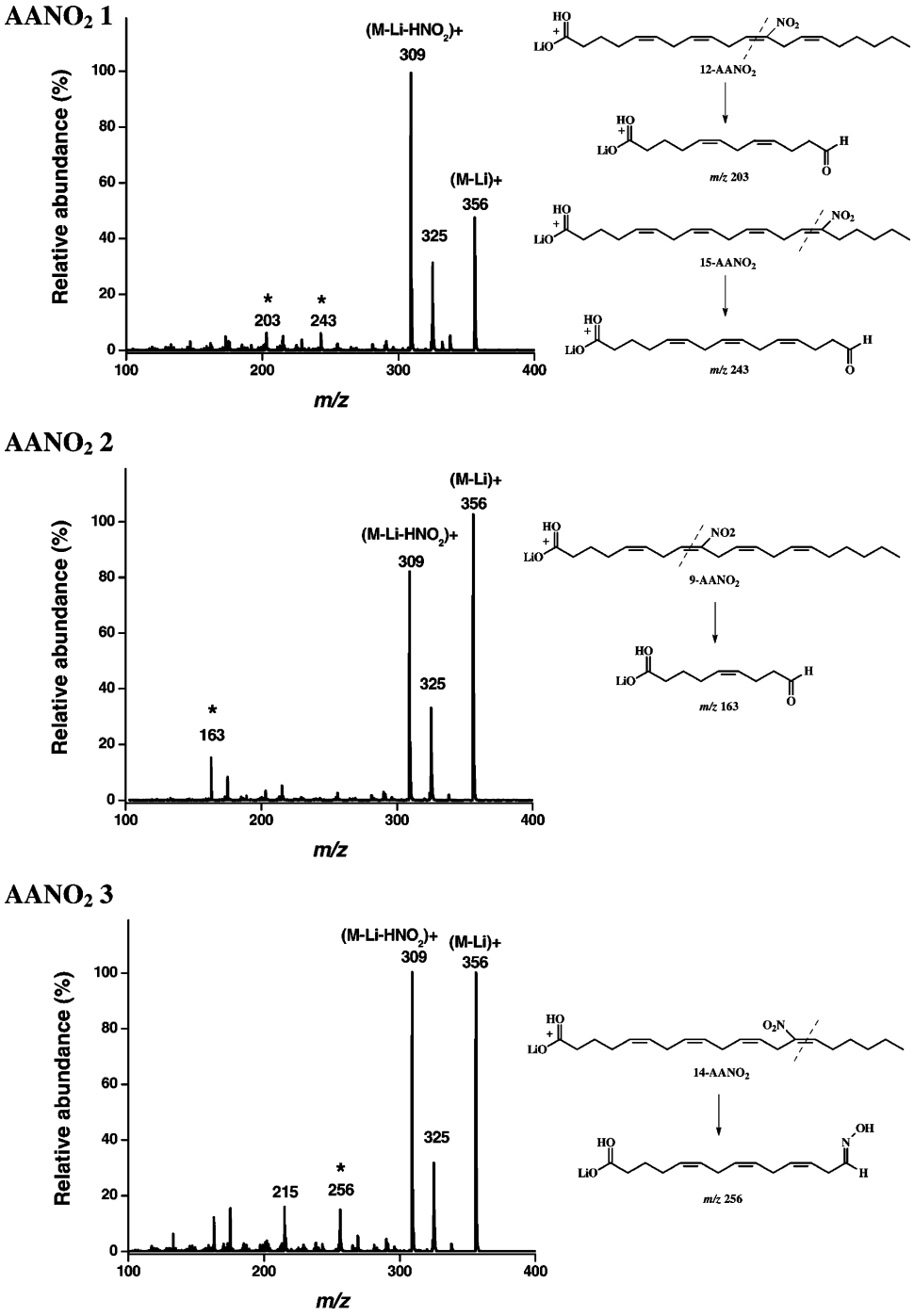


FIGURE 2: Mass spectrometry of lithium adducts of $AANO_2$. Lithium adducts of nitroalkene derivatives of AA were analyzed by MS in the positive mode as explained in Experimental Procedures. Product ion spectra of each purified fraction of $AANO_2$ is shown; major fragments corresponding to a specific isomer (as listed in Table 3) are marked with an asterisk.

dent manner by a mechanism that involved sGC since preincubation of the aortic rings with ODQ prevented vasorelaxation (Figure 3C). Maximal values of vasorelaxation were observed after 10 min of $AANO_2$ administration (see inset Figure 3C).

*Modulation of Macrophage Activation by $AANO_2$.* It has been well-established that AA signaling cascades and •NO pathways are related (*31*). In this way, we decided to evaluate the ability of $AANO_2$ to exert anti-inflammatory actions during macrophage activation by looking for NOS2 induction. Murine macrophages were activated with LPS/IFN$\gamma$, and NOS2 induction was followed by •NO production and Western blot (Figures 4A and 4B). When cells were activated, micromolar levels of $AANO_2$ caused a reduction of •NO generation that was maximal at 5 $\mu$M (Figure 4A). To assess the mechanism of NOS2 inhibition, the well-known transcriptional inhibitor cycloheximide was introduced in the system. While cycloheximide decreased •NO production in activated macrophages, $AANO_2$ was unable to further decrease •NO when added after cycloheximide (Figure 4A). These results suggest a transcriptional effect of the nitrolipid rather than acting on NOS2 synthesis/activity. Western blot analysis confirmed that NOS2 protein levels were lower in the presence of $AANO_2$ than in controls (Figure 4B). In addition, we investigated if •NO released during macrophage activation could have an inhibitory impact on NOS2 activity.

Table 3: Theorical Fragmentation Pattern of $AANO_2$−Lithium Adducts

| | Isomer | m/z of [M-H] | m/z of fragment (II) lithium derived | m/z of fragment (I) lithium derived |
|---|---|---|---|---|
| 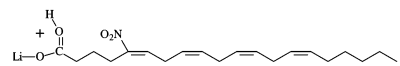 | 5- nitroAA | 356 | 136 | - |
| 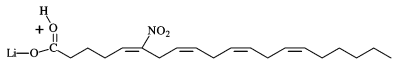 | 6- nitroAA | 356 | - | 123 |
| 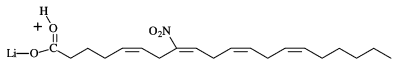 | 8- nitroAA | 356 | 176 | - |
| 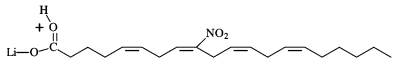 | 9- nitroAA | 356 | - | 163 |
| 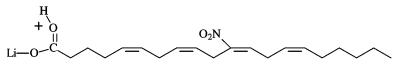 | 11- nitroAA | 356 | 216 | - |
| 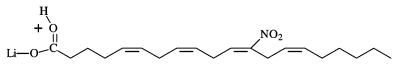 | 12- nitroAA | 356 | - | 203 |
| 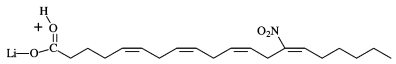 | 14- nitroAA | 356 | 256 | - |
| 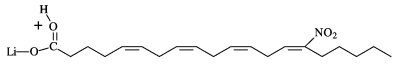 | 15- nitroAA | 356 | - | 243 |

The •NO− donor NOC-18 did not decrease •NO generation by activated macrophages (0.1−50 $\mu$M, Figure 4A), confirming that down-regulation of NOS2 expression was not associated with •NO released during $AANO_2$ decay.

## DISCUSSION

Herein, four major isomers of $AANO_2$ (9-, 12-, 14-, and 15-$AANO_2$) were identified, which exhibited key anti-inflammatory properties, including their ability to release biologically relevant fluxes of •NO, induce cGMP-dependent vasorelaxation, and modulate macrophage activation and NOS2 expression.

The addition of a $NO_2$ group to the AA carbon chain is indicated by the presence of an ion having *m*/*z* 348 in the MS negative ion mode. However, MS spectra cannot distinguish between a $-NO_2$ or a −ONO functional group. The identity of the functional group was solved by IR spectroscopy: the IR spectrum of $AANO_2$, in contrast to AA, exhibited absorbance maxima at 1370 and 1555 $cm^{-1}$ that correspond to a $-NO_2$ group of a nitroalkene attached to the carbon chain (Table 1 and Supporting Information). Since AA has four *cis*-double bonds, eight positional nitroalkene isomers can be formed from the addition of a nitro group to AA at the double bonds (Table 3). To elucidate which nitrated isomers were obtained in our experimental conditions, we used a novel MS methodology using lithium. This method is based on the remote-induced decompositions of lithium adducts of unsaturated fatty acid that have been used before to obtain structural information of unnitrated fatty acids (*32*). The presence of lithium allows the fragmentation of $AANO_2$ at the double bond yielding theoretical daughter ions with specific *m*/*z* that can be detected by MS/MS in the positive mode (Table 3). The analysis of the HPLC purified fractions exhibited the presence of the corresponding ions for 9-, 12-, 14-, and 15-$AANO_2$, with the 12- and 15-$AANO_2$ coeluting in fraction one (Figure 2). $^1H-^{13}C$ NMR as well as COSY, HBMC, and HMQC analysis confirmed the IR and MS results (Scheme 1, Table 2, and Supporting Information), validating the use of this method to identify positional isomers of nitrated fatty acids. In the NMR structural elucidation, the nitro-neighboring olefinic protons, chemical shifts near 7.00 ppm were used to start the analysis. From these signals, using HMQC, HMBC, and COSY, we were able to identify the neighboring protons and carbons. Then, α-methylene protons of carboxylic acid with chemical shifts near 2.40 ppm were used to analyze the head's protons of the molecule. Finally, the methyl protons of the molecule, chemical shifts near 0.90 ppm, together with COSY experiments allow us to construct the structure of the molecule's tail. Table 2 gathered the 14-$AANO_2$ most relevant signals that allow us to elucidate its structure. In this case a triplet at 7.14 ppm (H-15), a neighbor nitroolefinic proton, was connected to a proton at 2.28 ppm (H-16) using multiplicity, coupling constants, and COSY. The nitroolefinic carbons were assigned by correlations on the HMQC and HMBC experiments. On the other hand, from the triplet at 2.40 ppm, corresponding to H-2, and using COSY, HMQC, and HMBC, the atoms on the molecule's head were analyzed. Finally, protons H-16 to H-20 were assigned using COSY confirming coupling between protons at $\delta = 7.14$ (H-15) and $\delta = 2.28$ (H-16) ppm. The elucidation of the structure of the other isomers was also confirmed by NMR (see Supporting Information). From the IR, NMR, and MS data we clearly demonstrated the presence of mononitrated nitroalkenes: 9-nitroicosa-5,8,11,14-tetraenoic acid (9-$AANO_2$), 12-nitroicosa-5,8,11,14-tetraenoic acid (12-$AANO_2$), 14-nitroicosa-

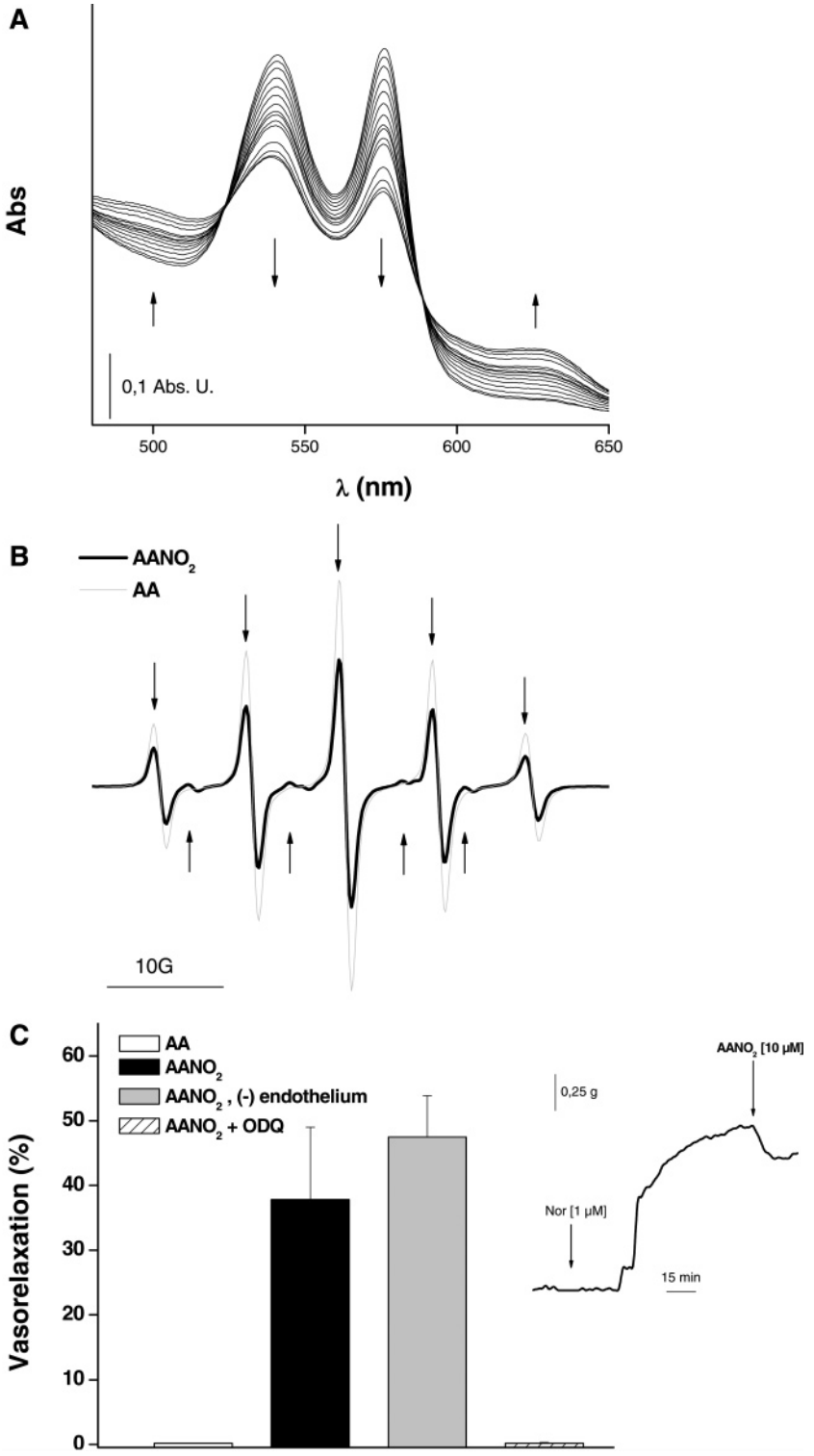


FIGURE 3: Biological activity of $AANO_2$. The capacity of nitroarachidonate (fraction 3) to release •NO was evaluated by oxyHb oxidation (A) and EPR (B). Similar results were obtained from fractions 1 and 2 (data not shown). The oxidation of oxyHb (20 $\mu$M) was followed recording the spectra at 5 min intervals following the increase in absorbance at 503 and 630 nm and the decrease at 540 and 577 nm characteristic of the formation of metHb. The reduction of cPTIO to cPTI by $AANO_2$ (300 $\mu$M, black line) was determined by EPR as explained in Experimental Procedures; control was performed using AA (300 $\mu$M, gray line). (C) Rat aortic vessels were precontracted with 1 $\mu$M NOR and then exposed to 10 $\mu$M $AANO_2$ with (black bar) or without endothelium (gray bar). Experiments were also performed after 15 min preincubation with ODQ (30 $\mu$M, dash bar). White bar: AA control. Data correspond to the mean ± SD, $n = 3$. Inset: representative trace of $AANO_2$-mediated vasorelaxation. At the indicated points NOR and $AANO_2$ were added.

5,8,11,14-tetraenoic acid (14-$AANO_2$) and 15-nitroicosa-5,8,11,14-tetraenoic acid (15-$AANO_2$).

Previous reports demonstrated that $AA(OH)NO_2$ is a bioactive compound that induces vasorelaxation due to its capacity to release •NO in a non-indomethacin-inhibitable mechanism (*7*). This is consistent with the reported formation of $AANO_2$ and $AA(OH)NO_2$ in healthy human plasma and urine (*16*). However, the capacity of $AANO_2$ to exert vasorelaxation and release •NO was not yet evaluated. Herein, we demonstrated the production of •NO from $AANO_2$ using

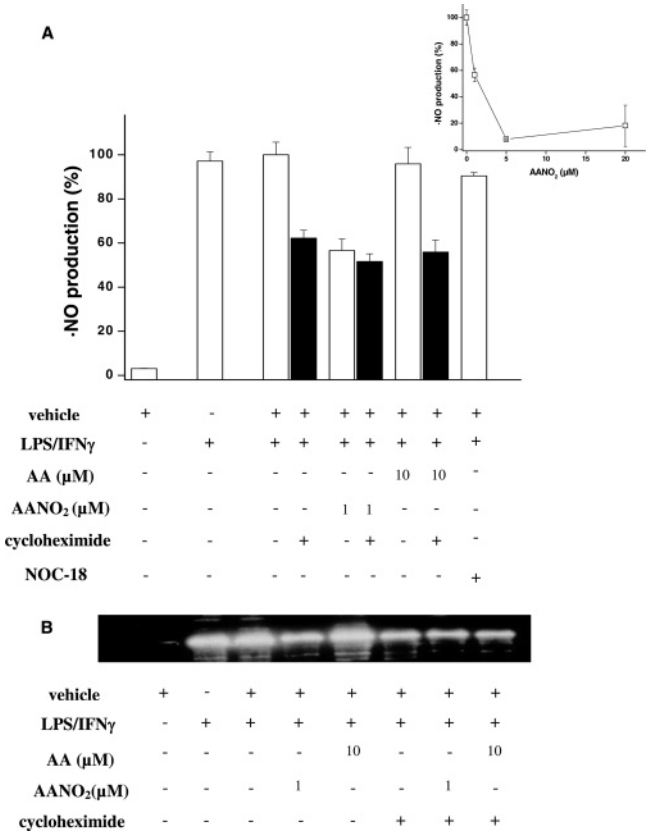


FIGURE 4: $AANO_2$ inhibited •NO generation by activated macrophages. (A) Mouse J774.1 macrophages were activated with LPS plus IFN$\gamma$; $AANO_2$ (a mixture of the four isomers) and non-nitrated AA were added together with the activating molecules (white bars); after 6 h incubation •NO was measured by fluorimetry using DAF-DA. As a control, •NO generation was also measured in the presence of NOC-18 (50 $\mu$M). •NO formation was also measured in the presence of cycloheximide (black bars) as explained in Experimental Procedures. Results are expressed as the mean of fluorescence units ± SD of triplicates. Results are representative of two independent experiments. Inset: Dose-dependent inhibition of •NO production by $AANO_2$. (B) Aliquots were taken from A and analyzed for NOS2 expression by Western blot.

different experimental approaches. The maximal observed release of •NO was about 8 $\mu$mol/mmol of $AANO_2$/min (0.8% of $AANO_2$), enough to explain its ability to activate sGC and induce vasorelaxation taking into account the already reported EC(50) for •NO (10 nM, ref *33*). Moreover, proving the participation of •NO in this process, the sGC inhibitor ODQ prevented $AANO_2$-induced vasorelaxation (Figure 3C). Nitric oxide detection from $AANO_2$ required the presence of SOD, indicating that $AANO_2$ decomposition involves the formation of $O_2^{\bullet-}$ that reacts with •NO to form peroxynitrite, thus decreasing •NO bioability. The mechanism of release of •NO by nitrated fatty acids is still controversial. While Schopfer, F., et al. proposed a modified Nef reaction mechanism (*13*), Lima, E., et al. suggested that •NO comes from the isomerization of the nitro fatty acid to the corresponding nitrite derivative through a homolytic scission and/or reduction of the $-NO_2$ group yielding a carbon-centered radical (*20*). Preliminary data show that a carbon-centered radical is formed in our system that can be responsible for the formation of $O_2^{\bullet-}$, which explains the need of SOD to detect •NO by the •NO electrode (data not shown).

It has been clearly demonstrated that free ($LNO_2$, $OANO_2$, refs *16*, *34*−*37*) as well as sterified (cholesteryl-nitrolinoleate[2]) nitroalkenes exert anti-inflammatory actions *via* PPAR$\gamma$ dependent and independent mechanisms. We analyzed the ability of $AANO_2$ to modulate monocyte/macrophage activation by inflammatory stimulus and found that $AANO_2$ down-regulated NOS2 induction in a dose-dependent manner (Figure 4). Inhibition of NOS2 synthesis was also demonstrated in experiments using cycloheximide, which stopped protein translation (Figure 4B). This suggests that the ability of $AANO_2$ to inhibit •NO generation was at the NOS2 induction level rather than affecting enzyme activity. Down-regulation of NOS2 by $AANO_2$ under inflammatory stimulus should contribute to the physiological shut down of the inflammatory response of macrophages. This anti-inflammatory action involves different pathways that occur at a transcriptional level, including NF-$\kappa$B and Nrf2 activation (Ferrari, M., et al., unpublished results). In summary, all major isomers of $AANO_2$ were able to release •NO and modulate macrophage activation. Future work will address which isomers predominate *in vivo* as novel anti-inflammatory footprints.

## ACKNOWLEDGMENT

We would like to thank Gonzalo Peluffo, Horacio Botti, Rafael Radi, and Bruce A. Freeman for helpful discussions and Carlos Batthyany, Virginia López, and Horacio Pezaroglo for technical assistance.

## SUPPORTING INFORMATION AVAILABLE

TLC data and MS, IR, and NMR primary spectra are provided. This material is available free of charge via the Internet at http://pubs.acs.org.

## REFERENCES

1. Rouzer, C. A., and Marnett, L. J. (2003) Mechanism of free radical oxygenation of polyunsaturated fatty acids by cyclooxygenases, *Chem. Rev. 103*, 2239−2304.
2. Goodwin, D. C., Landino, L. M., and Marnett, L. J. (1999) Effects of nitric oxide and nitric oxide-derived species on prostaglandin endoperoxide synthase and prostaglandin biosynthesis, *FASEB J. 13*, 1121−1136.
3. Di Rosa, M., Ialenti, A., Ianaro, A., and Sautebin, L. (1996) Interaction between nitric oxide and cyclooxygenase pathways, *Prostaglandins, Leukotrienes Essent. Fatty Acids 54*, 229−238.
4. Marnett, L. J. (2002) Recent developments in cyclooxygenase inhibition, *Prostaglandins Other Lipid Mediators* 68-*69*, 153−164.
5. Jiang, H., Kruger, N., Lahiri, D. R., Wang, D., Vatele, J. M., and Balazy, M. (1999) Nitrogen dioxide induces cis-trans-isomerization of arachidonic acid within cellular phospholipids. Detection of trans-arachidonic acids in vivo, *J. Biol. Chem. 274*, 16235−16241.
6. Salvemini, D., Currie, M. G., and Mollace, V. (1996) Nitric oxide-mediated cyclooxygenase activation. A key event in the antiplatelet effects of nitrovasodilators, *J. Clin. Invest. 97*, 2562−2568.
7. Balazy, M., Iesaki, T., Park, J. L., Jiang, H., Kaminski, P. M., and Wolin, M. S. (2001) Vicinal nitrohydroxyeicosatrienoic acids: vasodilator lipids formed by reaction of nitrogen dioxide with arachidonic acid, *J. Pharmacol. Exp. Ther. 299*, 611−619.
8. Goodwin, D. C., Gunther, M. R., Hsi, L. C., Crews, B. C., Eling, T. E., Mason, R. P., and Marnett, L. J. (1998) Nitric oxide trapping of tyrosyl radicals generated during prostaglandin endoperoxide

[2] Ferreira, A. M., Batthyany, C., Ferrari, M., Trostchansky, A., Souza, J. M., Alvarez, M. N., Lopez, V. G., Schopfer, F. J., O'Donnell, V. B., Freeman, B. A., and Rubbo, H., submitted for publication.

synthase turnover. Detection of the radical derivative of tyrosine 385, *J. Biol. Chem. 273*, 8903−8909.
9. Trostchansky, A., O'Donnell, V. B., Goodwin, D. C., Landino, L. M., Marnett, L. J., Radi, R., and Rubbo, H. (2007) Interactions between nitric oxide and peroxynitrite during prostaglandin endoperoxide H synthase catalysis: a free radical mechanism of inactivation, *Free Radical Biol. Med. 42*, 1029−1038.
10. Trostchansky, A., Batthyany, C., Botti, H., Radi, R., Denicola, A., and Rubbo, H. (2001) Formation of Lipid-Protein Adducts in Low-Density Lipoprotein by Fluxes of Peroxynitrite and Its Inhibition by Nitric Oxide, *Arch. Biochem. Biophys. 395*, 225−232.
11. Rubbo, H., Radi, R., Anselmi, D., Kirk, M., Barnes, S., Butler, J., Eiserich, J. P., and Freeman, B. A. (2000) Nitric oxide reaction with lipid peroxyl radicals spares alpha-tocopherol during lipid peroxidation. Greater oxidant protection from the pair nitric oxide/alpha-tocopherol than alpha-tocopherol/ascorbate, *J. Biol. Chem. 275*, 10812−10818.
12. Rubbo, H., Radi, R., Trujillo, M., Telleri, R., Kalyanaraman, B., Barnes, S., Kirk, M., and Freeman, B. A. (1994) Nitric oxide regulation of superoxide and peroxynitrite-dependent lipid peroxidation. Formation of novel nitrogen-containing oxidized lipid derivatives, *J. Biol. Chem. 269*, 26066−26075.
13. Schopfer, F. J., Baker, P. R., Giles, G., Chumley, P., Batthyany, C., Crawford, J., Patel, R. P., Hogg, N., Branchaud, B. P., Lancaster, J. R., Jr., and Freeman, B. A. (2005) Fatty acid transduction of nitric oxide signaling. Nitrolinoleic acid is a hydrophobically stabilized nitric oxide donor, *J. Biol. Chem. 280*, 19289−19297.
14. Lim, D. G., Sweeney, S., Bloodsworth, A., White, C. R., Chumley, P. H., Krishna, N. R., Schopfer, F., O'Donnell, V. B., Eiserich, J. P., and Freeman, B. A. (2002) Nitrolinoleate, a nitric oxide-derived mediator of cell function: synthesis, characterization, and vasomotor activity, *Proc. Natl. Acad. Sci. U.S.A. 99*, 15941−15946.
15. Lima, E. S., Di Mascio, P., and Abdalla, D. S. (2003) Cholesteryl nitrolinoleate, a nitrated lipid present in human blood plasma and lipoproteins, *J. Lipid Res. 44*, 1660−1666.
16. Baker, P. R., Lin, Y., Schopfer, F. J., Woodcock, S. R., Groeger, A. L., Batthyany, C., Sweeney, S., Long, M. H., Iles, K. E., Baker, L. M., Branchaud, B. P., Chen, Y. E., and Freeman, B. A. (2005) Fatty acid transduction of nitric oxide signaling: multiple nitrated unsaturated fatty acid derivatives exist in human blood and urine and serve as endogenous peroxisome proliferator-activated receptor ligands, *J. Biol. Chem. 280*, 42464−42475.
17. Lima, E. S., Di Mascio, P., Rubbo, H., and Abdalla, D. S. (2002) Characterization of linoleic acid nitration in human blood plasma by mass spectrometry, *Biochemistry 41*, 10717−10722.
18. Baker, P. R., Schopfer, F. J., Sweeney, S., and Freeman, B. A. (2004) Red cell membrane and plasma linoleic acid nitration products: synthesis, clinical identification, and quantitation, *Proc. Natl. Acad. Sci. U.S.A. 101*, 11577−11582.
19. Schopfer, F. J., Lin, Y., Baker, P. R., Cui, T., Garcia-Barrio, M., Zhang, J., Chen, K., Chen, Y. E., and Freeman, B. A. (2005) Nitrolinoleic acid: an endogenous peroxisome proliferator-activated receptor gamma ligand, *Proc. Natl. Acad. Sci. U.S.A. 102*, 2340−2345.
20. Lima, E. S., Bonini, M. G., Augusto, O., Barbeiro, H. V., Souza, H. P., and Abdalla, D. S. (2005) Nitrated lipids decompose to nitric oxide and lipid radicals and cause vasorelaxation, *Free Radical Biol. Med. 39*, 532−539.
21. Balazy, M., and Poff, C. D. (2004) Biological nitration of arachidonic acid, *Curr. Vasc. Pharmacol. 2*, 81−93.
22. O'Donnell, V. B., Eiserich, J. P., Chumley, P. H., Jablonsky, M. J., Krishna, N. R., Kirk, M., Barnes, S., Darley-Usmar, V. M., and Freeman, B. A. (1999) Nitration of unsaturated fatty acids by nitric oxide-derived reactive nitrogen species peroxynitrite, nitrous acid, nitrogen dioxide, and nitronium ion, *Chem. Res. Toxicol. 12*, 83−92.
23. Napolitano, A., Panzella, L., Savarese, M., Sacchi, R., Giudicianni, I., Paolillo, L., and d'Ischia, M. (2004) Acid-induced structural modifications of unsaturated Fatty acids and phenolic olive oil constituents by nitrite ions: a chemical assessment, *Chem. Res. Toxicol. 17*, 1329−1337.
24. Panzella, L., Manini, P., Crescenzi, O., Napolitano, A., and d'Ischia, M. (2003) Nitrite-induced nitration pathways of retinoic acid, 5,6-epoxyretinoic acid, and their esters under mildly acidic conditions: toward a reappraisal of retinoids as scavengers of reactive nitrogen species, *Chem. Res. Toxicol. 16*, 502−511.
25. Napolitano, A., Camera, E., Picardo, M., and d'Ishida, M. (2002) Reactions of hydro(pero)xy derivatives of polyunsaturated fatty acids/esters with nitrite ions under acidic conditions. Unusual nitrosative breakdown of methyl 13-hydro(pero)xyoctadeca-9,-11-dienoate to a novel 4-nitro-2-oximinoalk-3-enal product, *J. Org. Chem. 67*, 1125−1132.
26. Bligh, E. G., and Dyer, W. J. (1959) A rapid method of total lipid extraction and purification, *Can. J. Biochem. Physiol. 37*, 911−917.
27. Alexander, R. L., Bates, D. J., Wright, M. W., King, S. B., and Morrow, C. S. (2006) Modulation of Nitrated Lipid Signaling by Multidrug Resistance Protein 1 (MRP1): Glutathione Conjugation and MRP1-Mediated Efflux Inhibit Nitrolinoleic Acid-Induced, PPARgamma-Dependent Transcription Activation, *Biochemistry 45*, 7889−7896.
28. Murphy, R. C., Fiedler, J., and Hevko, J. (2001) Analysis of nonvolatile lipids by mass spectrometry, *Chem. Rev. 101*, 479−526.
29. Akaike, T., and Maeda, H. (1996) Quantitation of nitric oxide using 2-phenyl-4,4,5,5-tetramethylimidazoline-1-oxyl 3-oxide (PTIO), *Methods Enzymol. 268*, 211−221.
30. Lopez, G. V., Batthyany, C., Blanco, F., Botti, H., Trostchansky, A., Migliaro, E., Radi, R., Gonzalez, M., Cerecetto, H., and Rubbo, H. (2005) Design, synthesis, and biological characterization of potential antiatherogenic nitric oxide releasing tocopherol analogs, *Bioorg. Med. Chem. 13*, 5787−5796.
31. Salvemini, D., Seibert, K., Masferrer, J. L., Settle, S. L., Misko, T. P., Currie, M. G., and Needleman, P. (1995) Nitric oxide and the cyclooxygenase pathway, *Adv. Prostaglandin, Thromboxane, Leukotriene Res. 23*, 491−493.
32. Crockett, J. S., Gross, M. L., Christie, W. W., and Holman, R. T. (1990) Collisional activation of a series of homoconjugated octadecadienoic acids with fast atom bombardment and tandem mass spectrometry, *J. Am. Soc. Mass Spectrom. 1*, 183−191.
33. Roy, B., and Garthwaite, J. (2006) Nitric oxide activation of guanylyl cyclase in cells revisited, *Proc. Natl. Acad. Sci. U.S.A. 103*, 12185−12190.
34. Wright, M. M., Schopfer, F. J., Baker, P. R., Vidyasagar, V., Powell, P., Chumley, P., Iles, K. E., Freeman, B. A., and Agarwal, A. (2006) Fatty acid transduction of nitric oxide signaling: Nitrolinoleic acid potently activates endothelial heme oxygenase 1 expression, *Proc. Natl. Acad. Sci. U.S.A. 103*, 4299−4304.
35. Coles, B., Bloodsworth, A., Clark, S. R., Lewis, M. J., Cross, A. R., Freeman, B. A., and O'Donnell, V. B. (2002) Nitrolinoleate Inhibits Superoxide Generation, Degranulation, and Integrin Expression by Human Neutrophils: Novel Antiinflammatory Properties of Nitric Oxide-Derived Reactive Species in Vascular Cells, *Circ. Res. 91*, 375−381.
36. Batthyany, C., Schopfer, F. J., Baker, P. R., Duran, R., Baker, L. M., Huang, Y., Cervenansky, C., Branchaud, B. P., and Freeman, B. A. (2006) Reversible Post-translational Modification of Proteins by Nitrated Fatty Acids in Vivo, *J. Biol. Chem. 281*, 20450−20463.
37. Cui, T., Schopfer, F. J., Zhang, J., Chen, K., Ichikawa, T., Baker, P. R., Batthyany, C., Chacko, B. K., Feng, X., Patel, R. P., Agarwal, A., Freeman, B. A., and Chen, Y. E. (2006) Nitrated fatty acids: Endogenous anti-inflammatory signaling mediators, *J. Biol. Chem. 281*, 35686−35698.

BI602652J